Biophysical Chemistry 171 (2013) 16–23

Contents lists available at SciVerse ScienceDirect

Biophysical Chemistry

journal homepage: http://www.elsevier.com/locate/biophyschem

Dynamic control of the prolyl isomerase function of the dual-domain SlyD protein

Michael Kovermann, Jochen Balbach *

Institut für Physik, Biophysik, Martin-Luther-Universität Halle-Wittenberg, D-06099 Halle (Saale), Germany
Mitteldeutsches Zentrum für Struktur und Dynamik der Proteine (MZP), Martin-Luther-Universität Halle-Wittenberg, D-06099 Halle (Saale), Germany

HIGHLIGHTS

- The chaperone domain of the SlyD protein facilitates its high catalytic efficiency.
- We find a dynamic coupling of the two domains at various time scales.
- Inhibitor binding and point mutations modify the dynamics and catalysis.
- A proposed model connects the local dynamics to the steps of catalysis.

GRAPHICAL ABSTRACT

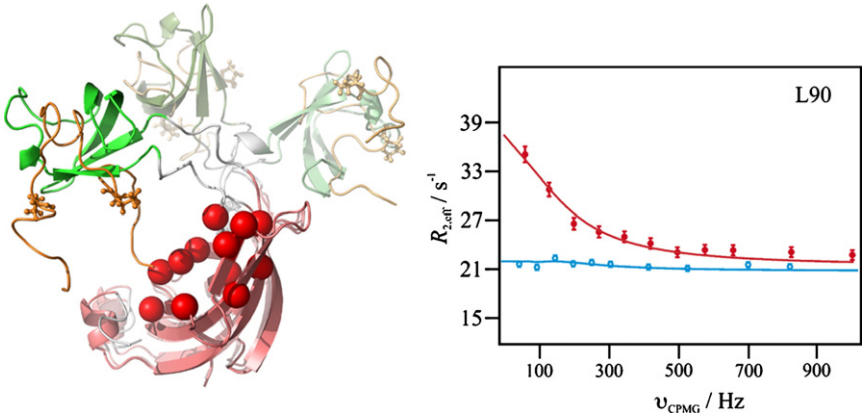

ARTICLE INFO

Article history:
Received 21 September 2012
Received in revised form 22 November 2012
Accepted 22 November 2012
Available online 8 December 2012

Keywords:
NMR
Fluorescence
PPIase
FKBP
Dynamics
Enzymology

ABSTRACT

Local dynamics on variable timescales are important to facilitate high catalytic efficiency in enzymes. In this study, we examined the dual-domain peptidyl-prolyl *cis*/*trans*-isomerase (PPIase) SlyD with regard to its catalytic cycle. Fluorescence- and NMR-based experiments were performed to understand the high catalytic efficiency of SlyD compared to single domain FKBP proteins. We probed local conformational changes for amino acids involved in substrate-binding (IF domain) and substrate-catalysis (FKBP domain) taking place on the timescale of substrate turnover. Binding of the PPIase activity inhibitors to the FKBP domain suppressed the conformational freedom of the remote IF domain. A single side-chain mutation in the active site strongly reduced the rate of substrate turnover and changed the conformational dynamics of all amino acids involved in catalysis. This dynamic interplay between substrate-binding domain and PPIase domain determines the high catalytic activity of SlyD and inhibitor-binding modulates the backbone plasticity required for enzyme activity.

1. Introduction

SlyD (sensitive to *lysis D*), first discovered in *Escherichia coli* (*E. coli*) [1], belongs to the family of peptidyl-prolyl *cis*/*trans*-isomerases (PPIase) and metallochaperones [2,3] and has been well characterized in terms of its biological functions [4–9] and structural biology [10–12]. SlyD is involved in bacterial Tat (twin-arginine translocation) transport of folded proteins across the cytoplasmic membrane and is required during the maturation of urease and [NiFe]-hydrogenase for nickel insertion. High resolution NMR investigations of full-length *E. coli* SlyD [11], of a C-terminally truncated variant 1–165 [12], *Ec*SlyD*, of a C-terminally truncated *Heliobacter pylori* SlyD [13] and of a combined X-ray/SAXS study of a full-length SlyD homologue isolated from a thermophile [10], *Tt*SlyD, clearly showed an overall fold typical of two

* Corresponding author at: Institut für Physik, Fachgruppe Biophysik, Martin-Luther-Universität Halle-Wittenberg, Betty-Heimann-Str. 7, D-06120 Halle (Saale), Germany. Tel.: +49 345 55 28550; fax: +49 345 55 27161.
E-mail address: jochen.balbach@physik.uni-halle.de (J. Balbach).

0301-4622/$ – see front matter © 2012 Elsevier B.V. All rights reserved.
http://dx.doi.org/10.1016/j.bpc.2012.11.003

domains, which is congruent with a loose domain–domain orientation [11,12].

The FKBP domain contains the PPIase active site [2,5,14,15], and is structurally similar to *h*FKBP12 [16,17]. The other so-called IF (insert in flap) domain [18], harbors the chaperone function [19–21]. Folding and stability studies of different SlyD variants showed that both kinetic and thermodynamic parameters strongly depend on the presence or absence of both domains [10,22]. Interaction studies of SlyD with partially folded and unfolded peptides (such as Suc-ALPF-pNA [23] and Tat signal peptides [9,24]), as well as permanently unfolded proteins (such as RCM-T1 and RCM-α-lactalbumin), observed via fluorescence or NMR spectroscopy, showed distinct binding sites in the IF and/or in the FKBP domain [10,12,25]. Additionally, far-UV CD and ITC methods showed metal binding of *Ec*SlyD [11] and the binding site could be resolved in the crystal structure of *Tt*SlyD [10]. Kaluarachchi et al. [7] observed the quantitative coordination of up to seven Ni(II) ions to one *Ec*SlyD molecule via mass spectrometry and the essential role of C-terminal residues 166–196 for full in vivo function during hydrogenase maturation [8,13,26].

Recent NMR dynamics reports on a ps-to-ns timescale of free and peptide-bound mesophilic and thermophilic SlyD [25] suggested a dynamic coupling between the PPIase and IF domains. Single molecule fluorescence energy transfer (smFRET) measurements confirmed a structural heterogeneity of native *Tt*SlyD [27] corresponding to an open and closed conformation. These conformations interconvert with a rate constant of about 100 s^{-1}, which corresponds to the rate-limiting product dissociation rate [28]. Both conformations and this interconversion rate were observed for both free and substrate-bound *Tt*SlyD [27]. Although probing the link between catalytic efficiency and substrate turnover using the intrinsic dynamics of an enzyme is of key interest [29–31], it is still challenging to analyze the time-dependent course of enzyme dynamics during substrate turnover. NMR spectroscopy offers the tools to investigate enzyme dynamics on ps to hour or even and day timescale [32–34]. Within the μs-to-ms timescale, which is about the timescale of catalysis, R_2 relaxation dispersion experiments [35–37] probe dynamic events on a residue-by-residue basis and allow interpretation of kinetic data in terms of global domain motion or enzymatic activity. Using this approach Eisenmesser and coworkers showed for the PPIase cyclophilin A (CypA) a strong correlation for the frequencies of protein motions within the substrate-free state and the corresponding catalytic turnover rates [31]. This observation could be refined using the temperature, the deuteration and the magnetic field strength dependency of the relaxation rate R_2 of wild type and CypA variants [38]. Relaxation dispersion experiments were used as well to monitor changes in ligand dynamics upon interaction to the PPIase Pin1 [39].

In the present study we investigated the dynamic coupling of the FKBP and IF domain and its link to the enzymatic activity of SlyD. Towards this end we used PPIase activity inhibitors modifying both substrate turnover and the domain dynamics. We used equilibrium and kinetic NMR and fluorescence experiments with inhibitors of isomerase activity, such as FK506 and Rapamycin, as well as ^{15}N R_2 relaxation dispersion experiments. These biophysical methods monitor conformational changes of amino acids responsible for peptidyl-prolyl *cis/trans* isomerization activity in both the FKBP domain and the remote IF domain. The here presented study with PPIase inhibitors confirms that during the catalytic enzyme mechanism of SlyD, opening and closing of the substrate-bound IF domain and the catalytic FKBP domain allow the sampling of suitable conformations 100 times faster compared to the rate-limiting substrate dissociation. These fluctuations are generic properties of free SlyD employed for its enzymatic function.

2. Materials and methods

2.1. Proteins, peptides and organic molecules

The expression and purification of *Ec*SlyD* as well as *Tt*SlyD were performed as described [10,12]. We used His-tag variants of a truncated version of *Ec*SlyD (*Ec*SlyD*, comprising residues 1–165) and full-length *Tt*SlyD (with residues 1–148), both purified by immobilized nickel ion affinity chromatography. In the case of *Tt*SlyDΔIF, residues 65–136 were replaced by the loop (ATGHPIIPPAHT) in analogy to the FKBP12 flap region [10]. *Ec*SlyD*Y68W was expressed and purified as *Ec*SlyD*, the point mutation was inserted by site-directed mutagenesis via QuikChange® (Stratagene).

For fluorescence titration experiments we used a 27 amino acid-long peptide with a twin arginine motif (NH_2-QRRDFLKYSVALGVASALPL WSRAVFA-OH), purchased from Activotec, Cambridge, UK. The organic molecules Rapamycin and FK506 were purchased from Tecoland Corporation, Edison, USA. Dimethyl sulfoxide (DMSO) was purchased from Roth (Karlsruhe, Germany). Expression and purification of the RNase T1 variant (S54G/P55N) were carried out as previously described [40]. The reduced and S-carboxymethylated (RCM) form of RNase T1 was prepared according to [41,42].

2.2. NMR spectroscopy

All NMR experiments were performed on a Bruker 600 Avance II (equipped with a room temperature TXI probe) and on a Bruker 800 Avance III (equipped with a CP-TCI cryoprobe) spectrometer. Protein spectra were measured in 50 mM sodium phosphate and 100 mM sodium chloride, pH 7.5, containing 10% (v/v) D_2O and at $T = 298$ K. Backbone resonance assignments of *Ec*SlyD* and *Tt*SlyD samples are known [10,12].

The protein concentrations were 1.4 mM (for ^{15}N R_2 relaxation dispersion measurement of free *Ec*SlyD*, free *Ec*SlyD*Y68W as well as free *Tt*SlyD), and 0.66 mM (for ^{15}N R_2 relaxation dispersion measurement of Rapamycin-bound *Tt*SlyD), respectively.

The ^{15}N single quantum R_2 relaxation dispersion data of the protein backbone at $T = 298$ K were collected at a magnetic field strength of 14.1 T (*Ec*SlyD*, *Ec*SlyD*Y68W, *Tt*SlyD) and 18.8 T (*Ec*SlyD*, *Ec*SlyD*Y68W, *Tt*SlyD, Rapamycin-bound *Tt*SlyD) in a series of ^{1}H–^{15}N TROSY-HSQC based data sets [43]. The constant time relaxation delay, T, was set to 30 ms to ensure that the peak intensity in the CPMG relaxation spectrum I is about 50% of the intensity in the reference spectrum I_0 [37]. The values for $R_{2,\mathrm{eff}}$ were calculated using Eq. (1)

$$R_{2,\mathrm{eff}} = \frac{1}{T}\ln\left(\frac{I_0}{I}\right). \tag{1}$$

The $R_{2,\mathrm{eff}}$ values were plotted against the CPMG field strength to obtain ^{15}N R_2 relaxation dispersion curves for individual amide proton cross peaks. The relaxation dispersion curves were analyzed with the general solution of a two-site exchange model (Eq. (2)), which is independent of the exchange time regime [44]

$$R_{2,\mathrm{eff}}(\tau_{CP}) = \frac{1}{2}\left(R_{2a} + R_{2b} + k_{ex} - \frac{1}{\tau_{CP}}\cosh^{-1}\left(D_+\cosh(\eta_+) - D_-\cos(\eta_-)\right)\right), \tag{2}$$

with:

$$D_\pm = \frac{1}{2}\left(\frac{\psi + 2\Delta\omega^2}{\sqrt{\psi^2+\phi^2}} \pm 1\right)$$

$$\eta_\pm = \frac{\tau_{CP}}{\sqrt{2}}\sqrt{\sqrt{\psi^2+\phi^2} \pm \psi}$$

$$\psi = (R_{2a} - R_{2b} - p_a k_{ex} + p_b k_{ex})^2 - \Delta\omega^2 + 4p_a p_b {k_{ex}}^2$$

$$\phi = 2\Delta\omega(R_{2a} - R_{2b} - p_a k_{ex} + p_b k_{ex})$$

$$\Delta\omega = 2\pi\Delta\nu.$$

R_{2a} and R_{2b} are the ^{15}N transverse relaxation rates of the exchanging states in the absence of any chemical exchange, p_a and p_b are the

equilibrium populations of the particular state, k_{ex} is the exchange rate constant between the two states a and b, $\Delta\omega$ is the ^{15}N chemical shift difference between state a as well as b and τ_{CP} the time between successive 180° pulses and therewith one half of the inverse CPMG field strength, ν_{CPMG}. The slow exchange limit [37] was additionally used for free *Ec*SlyD* and *Tt*SlyD because the $R_{2,eff}$ values show a slow decay and small oscillations at low CPMG field strengths:

$$R_{2a,eff}(\tau_{CP}) = R_{2a} + k_a - k_a \frac{sin(\Delta\omega\tau_{CP})}{\Delta\omega\tau_{CP}}, \quad (3)$$

with the forward rate constant k_a and $2\tau_{CP}$ as the time delay between successive 180° pulses.

The NMR titration experiments with inhibitors were carried out at $T = 298$ K and a magnetic field strength of 14.1 T by successive addition of small aliquots of FK506 or Rapamycin (stock solutions of 12.4 mM dissolved in DMSO). Complex formation was monitored by recording 2D $^{1}H–^{15}N$ fHSQC spectra [45]. Both NMR titrations were complete with an excess of the inhibitor and a maximum dilution factor of 10%. We followed the progression of the peak intensity by increasing the amount of the inhibitor (slow exchange limit between protein and inhibitor, Fig. S3). To exclude any DMSO buffer effect, a DMSO control titration of *Tt*SlyD was performed.

All recorded NMR spectra were processed using NMRPipe [46] and analyzed using NMRView [47].

2.3. Fluorescence spectroscopy

Fluorescence spectra were measured with a JASCO FP-6500 fluorescence spectrometer equipped with a temperature controlled cell holder. All experiments were carried out at $T = 298$ K in 50 mM sodium phosphate and 100 mM sodium chloride, pH 7.5. For determination of the dissociation constant, K_D, for FK506 or Rapamycin and *Tt*SlyD as well as *Tt*SlyDΔIF, the quench of the protein fluorescence emission was measured at 308 nm after excitation at a wavelength of 280 nm. The excess of FK506 or Rapamycin was eight- to tenfold at the endpoint of the particular titration. Samples were carefully stirred during the whole titration experiment. The recorded fluorescence intensity data were corrected for buffer and dilution. The normalized fluorescence intensity quench with increasing inhibitor concentration was analyzed according to [48]

$$F(c) = q\frac{p + nc + K_D - \sqrt{(p + nc + K_D)^2 - 4npc}}{2p}, \quad (4)$$

where q is the maximum of the fluorescence quench, p is the concentration of the protein during titration experiment, c is the concentration of the inhibitor, n is the stoichiometry of binding and K_D is the dissociation constant of the binding process.

2.4. Stopped flow kinetic experiments

A sequential mixing stopped-flow spectrometer (Applied Photophysics) was used for all kinetic experiments. The reaction kinetics of the immunosuppressant-binding to the protein was observed by the change in fluorescence intensity using a cut-off filter of 305 nm after excitation at a wavelength of 280 nm. All experiments for the determination of association and dissociation behavior were carried out in 50 mM sodium phosphate and 100 mM sodium chloride, pH 7.5, at $T = 298$ K. The temperature of the whole mixing device was maintained with a circulating water bath. Inhibition reactions were initiated by a rapid 1:10 mixing of different concentrations of Rapamycin with a solution containing 2.3 μM *Tt*SlyD to obtain *pseudo* first-order conditions [49,50]. The same experimental procedure was repeated for *Tt*SlyDΔIF.

A tenfold excess of Rapamycin relative to the protein concentration in the mixing cell was used for recording Arrhenius-like behavior of the inhibition process. An additional control mixing experiment was performed to exclude any effect of DMSO on the buffer. No influence to fluorescence emission was observed. Kinetic time traces were collected at least seven times under identical conditions and were averaged for the fitting procedure according to Eq. (5),

$$I(t) = I_0 \exp(-Rt), \quad (5)$$

where I is the fluorescence emission intensity and R is the apparent rate constant for the inhibition event.

3. Results

3.1. Immunosuppressants FK506 and Rapamycin bind to the PPIase domain of TtSlyD

The macrolide peptides FK506 and Rapamycin [51,52] are prominent inhibitors for PPIases of the FKBP protein family [53–55]. The interaction between *Tt*SlyD and each inhibitor was followed on a residue-by-residue basis by NMR equilibrium titration experiments. The PPIase inhibitors were dissolved in DMSO because of water insolubility of FK506 and Rapamycin. An additional control titration of DMSO to *Tt*SlyD showed no significant disturbance for $^{1}H–^{15}N$ NMR cross peaks of *Tt*SlyD. A series of $^{1}H–^{15}N$ HSQC spectra of *Tt*SlyD with increasing amounts of the respective immunosuppressant FK506 or Rapamycin (Fig. S1 and S2 in the Supporting Material) showed that the FKBP domain of *Tt*SlyD was exclusively affected by adding the respective immunosuppressant (Fig. 1, *A* and *B*). With one exception (Asn 99 was closest to the binding pocket), the IF domain of *Tt*SlyD was not involved in interaction with the inhibitor. This is in contrast to recently reported data for SlyD from *E. coli* and in ethanol dissolved inhibitors [11], where chemical shift perturbations of residues comprising both domains were observed. Additionally, these conditions caused some sample precipitation, which we did not observe for *Tt*SlyD. Binding rates of Rapamycin or FK506 and *Tt*SlyD were slow compared to the NMR chemical shift timescale. G39 and Q16 (FKBP domain) or V113 and V115 (IF domain) for example are indicative for this timescale and for the domain-specific interaction. They show decreasing and increasing intensities at fixed chemical shift positions upon titration for the free and bound state, respectively (Fig. S3).

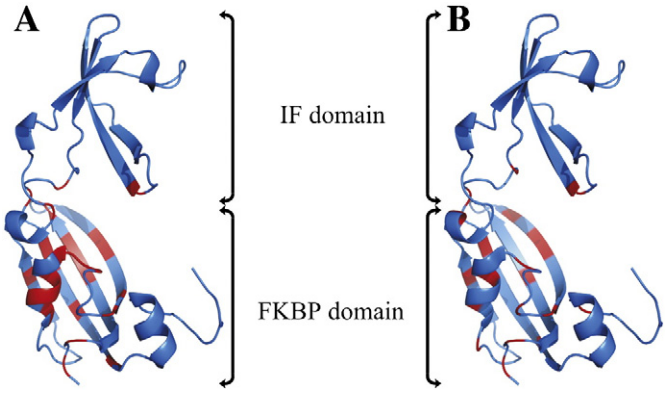

Fig. 1. NMR titration results of *Tt*SlyD with (*A*) FK506 and (*B*) Rapamycin. Residues experiencing an intensity loss upon inhibitor binding are colored in red in the crystal structure of *Tt*SlyD (3CGM.pdb) [10]. Binding occurs predominantly at the indicated FKBP domain.

3.2. The IF domain of TtSlyD decreases the inhibitor affinity

We determined the dissociation constant, K_D, and the stoichiometry, n, for the interaction of FK506 or Rapamycin to *Tt*SlyD as well as *Tt*SlyDΔIF (an IF domain-deficient variant) via fluorescence equilibrium titration experiments (Table 1 and Fig. S4, *A*–*D*). Although the IF domain shows no direct contact to the inhibitors (Fig. 1, *A* and *B*), the K_D value reveals a higher affinity of FK506 or Rapamycin to *Tt*SlyDΔIF compared to the full-length protein *Tt*SlyD. Moreover, the binding between FK506 and both *Tt*SlyD variants is stronger (up to 10 times) compared to Rapamycin. The stoichiometry, n, was two for Rapamycin binding and one for FK506 binding, indicating a 1:2 complex (Rapamycin) and a 1:1 complex (FK506), respectively. Binding of FK506 or Rapamycin to FKBP12 was in the nanomolar affinity range [53].

3.3. The presence of a binding partner for the IF domain strongly influences Rapamycin binding to the PPIase domain of TtSlyD

During the Tat-dependent translocation of folded substrates from the cytosol to the periplasm of *E. coli*, SlyD interacts with the unstructured Tat signal peptide of the substrate, protecting it from proteolytic degradation in the cytosol [9]. Previous NMR- and fluorescence-based binding studies showed that Tat signal peptides [9,23] only interact with the IF domain of SlyD [10,12,25]. We followed the binding of Rapamycin to *Tt*SlyD in the absence and presence of the Tat signal peptide (1–27) (Table 1). The dissociation constant, K_D, strongly increased at $T = 298$ K from 9.2 ± 0.1 μM up to 58 ± 1 μM (*solid circles* in Fig. S5) compared to the Rapamycin titration to *Tt*SlyD in the absence of the Tat peptide (1–27) (*open circles* in Fig. S5).

3.4. The IF domain limits association of Rapamycin to TtSlyD

Time-resolved fluorescence spectroscopy with a stopped-flow setup was used to determine the apparent association rate constant of Rapamycin to *Tt*SlyD, as well as to *Tt*SlyDΔIF, on a millisecond timescale. Interestingly, the binding of Rapamycin to *Tt*SlyDΔIF (*solid circles* in Fig. 2) was 3–4 times faster compared to full-length *Tt*SlyD (*open circles* in Fig. 2). This was the case for the entire temperature range analyzed. The slope in the two Arrhenius plots, and thus the activation energy, E_A, for the inhibition process was similar for both variants (straight lines in Fig. 2 correspond to $E_A = 60 \pm 3$ kJ mol^{-1}).

The kinetic stopped-flow experiments were extended by recording Rapamycin concentration-dependent fluorescence decay to obtain the association and dissociation rates for the binding of the inhibitor to *Tt*SlyD (*open circles* in Fig. 3) as well as *Tt*SlyDΔIF (*solid circles* in Fig. 3). Linear regression of the recorded apparent association rate constants k_{app} resulted in the same dissociation rate constant k_{off} of 25 ± 2 s^{-1} of Rapamycin for both *Tt*SlyD and *Tt*SlyDΔIF. In contrast, the association rate constant, k_{on}, differed. The presence of the IF domain reduced the rate of binding of Rapamycin to *Tt*SlyD by almost one order of magnitude ($k_{on} = 2.2 \pm 0.1$ μM^{-1} s^{-1} for *Tt*SlyD and $k_{on} = 14.9 \pm 0.7$ μM^{-1} s^{-1} for *Tt*SlyDΔIF). The K_D values (and therefore also the stoichiometry $n = 2$) determined for Rapamycin binding to *Tt*SlyD as well as to *Tt*SlyDΔIF observed with equilibrium fluorescence spectroscopy at $T = 298$ K (9.2 ± 0.2 μM as well as 1.7 ± 0.1 μM) confirmed the values determined by kinetic stopped-flow fluorescence data (11.4 ± 0.5 μM as well as 1.7 ± 0.1 μM). The release of the inhibitor, k_{off}, was faster compared to the substrate turnover, k_{cat}, and was not dependent on the presence of the IF domain.

Table 1
Dissociation constants K_D (per μM) for Rapamycin and FK506 interaction to *Tt*SlyD, *Tt*SlyDΔIF and Rapamycin interaction to *Tt*SlyD-Tat peptide (1–27) complex.

T/K	Rapamycin*			FK506*	
	*Tt*SlyD	*Tt*SlyDΔIF	*Tt*SlyD-Tat	*Tt*SlyD	*Tt*SlyDΔIF
298.2	9.2 ± 0.2	1.7 ± 0.1	58 ± 1	1.3 ± 0.1	0.20 ± 0.05

* The stoichiometry n of 2:1 (Rapamycin) and 1:1 (FK506) was kept constant during the fitting procedure for all variants.

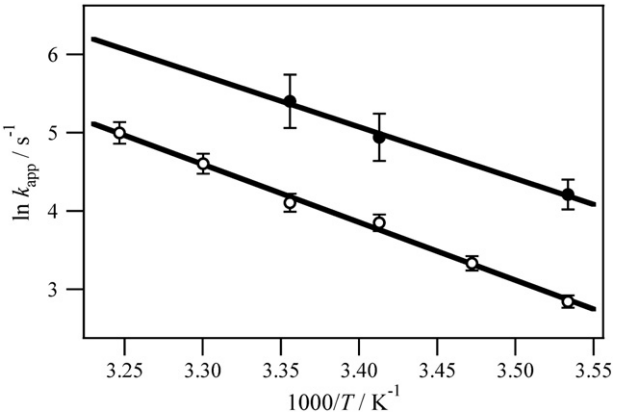

Fig. 2. Determination of the activation energy for association of the inhibitor to *Tt*SlyD and to *Tt*SlyDΔIF. Arrhenius representation of the apparent rate constant, k_{app}, for binding of Rapamycin to *Tt*SlyD (*open circles*) and to *Tt*SlyDΔIF (*solid circles*) determined by stopped-flow fluorescence spectroscopy. Fitting of a linear function to both kinetic data sets led to comparable slopes with a particular activation energy for inhibitor association of 60 ± 3 kJ mol^{-1} at $T = 298$ K.

3.5. Probing μs-to-ms dynamics of SlyD

To investigate the conformational dynamics of *Ec*SlyD*, *Ec*SlyD* Y68W, *Tt*SlyD and Rapamycin-bound *Tt*SlyD on a μs-to-ms timescale, we determined the contributions of chemical exchange, R_{ex}, to the ^{15}N transversal relaxation rates by R_2 relaxation dispersion experiments [36,37]. Almost all of the amino acids of the IF domain of the free state of *Ec*SlyD* (L75-D120) as well as of *Tt*SlyD (Q72-F117) sense a chemical exchange process at this timescale by revealing an R_{ex} contribution above 2 s^{-1}. Additionally, amino acids identified as being crucial for PPIase activity [10,56] (present in the FKBP domain), participate in dynamic events on the same timescale. All amino acids that sense this conformational exchange process are mapped on the structures of *Ec*SlyD* and *Tt*SlyD in Fig. 4, *A* and *B*. Note that these sensitive residues correspond exactly to residues that showed chemical shift changes upon peptide substrate binding of Suc-ALPF-pNA to *Ec*SlyD* [12].

Representative R_2 dispersion curves for four residues of free *Tt*SlyD are depicted in Fig. 5 (*open blue circles*). The regression of the Carver–

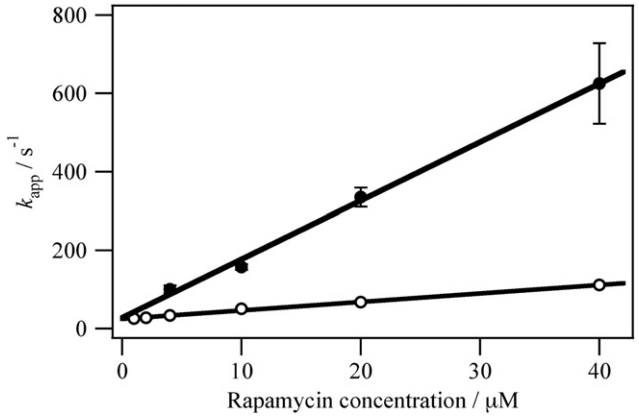

Fig. 3. Kinetic stopped-flow data analysis of binding of inhibitor to *Tt*SlyD and to *Tt*SlyDΔIF. The apparent rate constant, k_{app}, for binding of Rapamycin to *Tt*SlyD (*open circles*) and to *Tt*SlyDΔIF (*solid circles*) is depicted depending on the Rapamycin concentration. Linear extrapolation of the apparent rates k_{app} to 0 μM Rapamycin at $T = 298$ K revealed a unique k_{off} value of about 25 s^{-1} for both SlyD variants, whereas k_{on} values differed between *Tt*SlyD (2.2 ± 0.1 μM^{-1} s^{-1}) and *Tt*SlyDΔIF (14.9 ± 0.7 μM^{-1} s^{-1}).

Richards equation to the ^{15}N R_2 relaxation dispersion data of *Ec*SlyD*, as well as *Tt*SlyD with different starting parameters according to Eq. (2), consistently led to k_{ex} and $\Delta\omega$ values that indicated chemical exchange on the very slow NMR timescale ($k_{ex} \ll \Delta\omega$). Due to the small dispersion amplitude, reliable k_{ex} and population data are difficult to obtain. Global data regression of R_2 rates at two magnetic fields and of several amino acids simultaneously suggested k_{ex} data in the order of 1–10 s^{-1} and a ratio of populations of about 0.95:0.05. This exchange rate does not represent the global folding and unfolding rates of *Tt*SlyD or *Ec*SlyD* [22]. Therefore, application of the slow exchange limit according to Eq. (3) was justified leading to consistent k_a and $\Delta\omega$ values. Fig. S6 (*A*) presents individual dispersion curves for all those residues of *Ec*SlyD* which show an exchange contribution to R_2 above 2 s^{-1} (see Fig. 4 (*A*); corresponding fit statistics are listed in Table S1). The mean value for k_a individually determined for each of the 30 residues of *Ec*SlyD* showing R_2 dispersion is 3.7 ± 1.7 s^{-1} for all 30 residues. A global fit of the R_2 dispersion curves of these 30 residues revealed a value of 4.0 ± 0.2 s^{-1}, indicating concerted motion on this time scale.

3.6. Point mutation in the active site of *Ec*SlyD* strongly changes the μs-to-ms dynamics

The solution structure of *Ec*SlyD* showed that tyrosine 68 points towards the active site and partially fills the hydrophobic cleft [12]. Therefore Y68 might be responsible for the lower PPIase activity of the isolated FKBP domain of *Ec*SlyD* compared to FKBP12 [4]. An amino acid exchange of Y68 to a tryptophan, *Ec*SlyD*Y68W, reduced the catalytic rate constant for substrate turnover, k_{cat}, for the refolding of a standard protein substrate (RCM-T1 [41]) by a factor of 30 whereas the substrate affinity, K_M, was not influenced by this substitution (Table S2).

Interestingly, the μs-to-ms dynamics of the entire *Ec*SlyD*Y68W protein dramatically changed compared to *Ec*SlyD* (*solid red circles* in Fig. 6). The chemical exchange contribution R_{ex} increased to about 10–15 s^{-1} compared to 2 s^{-1} observed for *Ec*SlyD* (*open blue circles* in Fig. 6). Note, that IF domain, comprising amino acids that are distant to the mutation site in the FKBP domain, also sensed this higher chemical exchange (represented by V87, L90 and H116 in Fig. 6). The regression of the Carver–Richards equation to the ^{15}N R_2 relaxation dispersion data of *Ec*SlyD*Y68W led to significantly higher exchange rates, k_{ex}, of about 10^2–10^3 s^{-1} compared to *Ec*SlyD* but comparable population ratios for the two exchanging states (Fig. S7 provides exemplary data of *Ec*SlyD*Y68W at two magnetic fields for global data regression according to Eq. (2)).

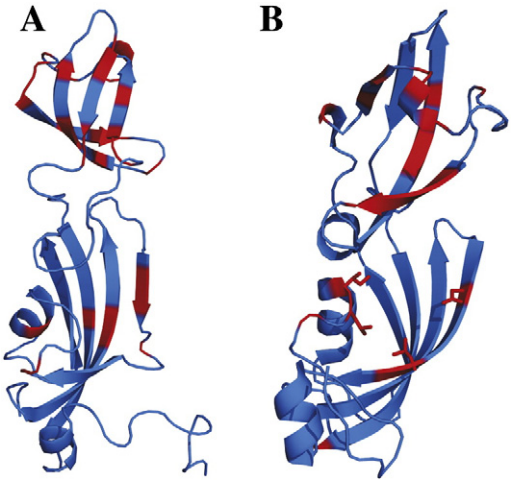

Fig. 4. Mapping of the ^{15}N R_2 relaxation dispersion results on the structure of (*A*) *Ec*SlyD* and (*B*) *Tt*SlyD at $T = 298$ K and a magnetic field strength of 18.8 T. Residues that experience R_{ex} contributions to R_2 above 2 s^{-1} are indicated in red. In (*B*) these residues are additionally marked by the side chain for those residues, which are contacted by the PPIase substrate in the FKBP domain in the crystal structure of *Tt*SlyD when in complex with a substrate peptide containing a proline [10].

3.7. The μs-to-ms dynamics of the IF domain of *Tt*SlyD are changed in the presence of Rapamycin

We also applied ^{15}N R_2 relaxation dispersion experiments to inhibitor-bound *Tt*SlyD to probe changes in the conformational dynamics observed in the free state of *Tt*SlyD. Surprisingly, Rapamycin led to a drastic change in the μs-to-ms dynamics of residues in the IF domain. Note that Rapamycin binds exclusively to the FKBP domain (Fig. 1 *B*). Amino acids that clearly sense conformational fluctuations in free *Tt*SlyD (*open blue circles* in Fig. 5) lose the dispersion of the ^{15}N $R_{2,eff}$ rates upon Rapamycin binding to the FKBP domain of *Tt*SlyD (*solid red circles* in Fig. 5). This change in motion could be caused by changes in the exchange rate, by disappearance of the chemical shift difference or highly diverse populations of the exchanging states.

4. Discussion

The high catalytic efficiency of the peptidyl-prolyl *cis*/*trans*-isomerase and metallochaperone SlyD is attributable to active inter-domain communication between the FKBP and IF domain. The molecular mechanism underlying this enzymatic catalysis has been previously investigated by various biophysical methods [10,22,57] including NMR [25] and single-molecule FRET experiments [27] which led to the following model. Apo-SlyD exists in open and closed conformations with respect to the domain orientation, and these conformations exchange at a rate of about 100 s^{-1}. This rate is independent of bound substrates or inhibitors. Initial binding of protein substrates to be catalyzed occurs at the IF domain. The closing reaction localizes the substrate close to the active site in the FKBP domain, which catalyzes the prolyl isomerization. The k_{cat} value corresponding to the rate of substrate dissociation is about 1 s^{-1}. Therefore, on average 100 opening and closing reactions take place before substrate release, which allows the probing of different substrate conformations and orientations in the proximity of the active site of the PPIase. This sampling is much less efficient in the absence of the IF domain due to random diffusion and thermal fluctuations resulting in a 200-fold drop in catalytic efficiency of SlyDΔIF.

This model could be confirmed and further refined (Fig. 7) by the here presented biophysical experiments following SlyD inhibition with the immunosuppressants FK506 and Rapamycin. Both interact only with the FKBP domain, which was confirmed by NMR titration experiments and chemical shift analysis. The dissociation constants for SlyD complexes with these inhibitors were reduced 5- to 7-fold in the absence of the IF domain. Therefore, we conclude that the IF domain in the closed form sterically hinders access to the active site of SlyD (Fig. 7). This steric hindrance can be amplified by presenting a binding partner to the IF domain. Additionally, kinetic experiments for binding of Rapamycin to *Tt*SlyDΔIF and to the native protein monitored by the intrinsic tryptophan fluorescence revealed 7-fold higher association rate constants, k_{on}, for *Tt*SlyDΔIF (15 μM^{-1} s^{-1}) compared to native *Tt*SlyD (2 μM^{-1} s^{-1}). The dissociation rate constants, k_{off}, for these two variants are the same (each about 25 s^{-1}). Again, we conclude that the spatial accessibility for inhibitor binding to the FKBP domain is limited in the presence of the IF domain. The opening and closing of the native protein are about 50-fold faster compared to the association rate at the protein concentrations used. As mentioned, Rapamycin binding neither changed the population nor the exchange rate of open and closed SlyD in smFRET experiments [27].

The ^{15}N R_2 NMR relaxation dispersion is caused by a slow chemical exchange process, with exchange rates between two states in the order of 1–10 s^{-1}. This timescale is very close to the enzymatic activity of SlyD* [4], with a k_{cat} value of about 1 s^{-1}. Two sets of residues sense

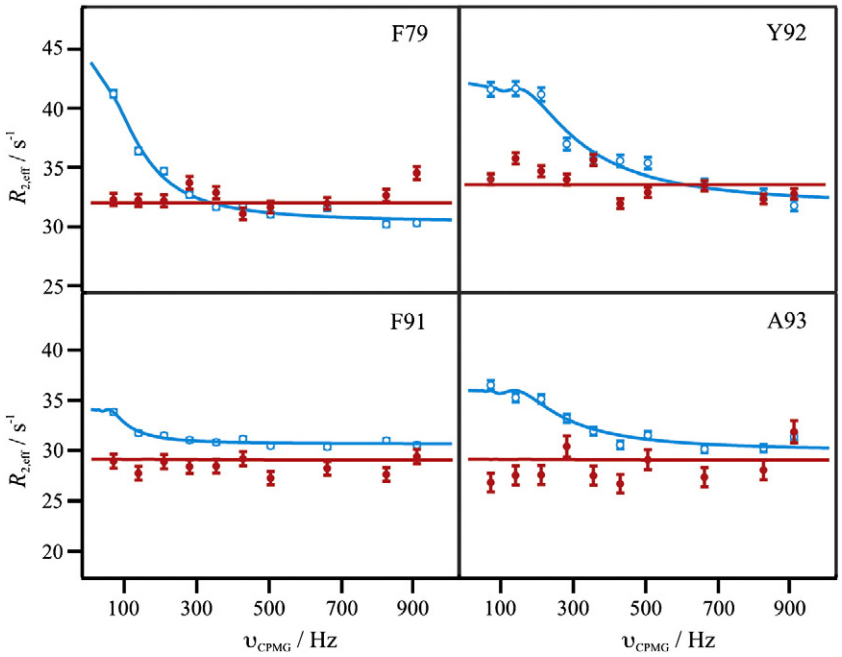

Fig. 5. Representative ^{15}N R_2 relaxation dispersion curves for free *Tt*SlyD (*open blue circles*) and the Rapamycin-bound state of *Tt*SlyD (*solid red circles*) are depicted for F79, Y92, F91 and A93 of the IF domain. Chemical exchange contributions, R_{ex}, of these amino acids are strongly suppressed upon inhibitor-binding although Rapamycin exclusively interacts with the FKBP domain (Fig. 1 *B*). The presented effective transversal relaxation rates, $R_{2,eff}$, were recorded at $T = 298$ K and a magnetic field strength of 18.8 T.

this exchange process (Fig. 4, *A* and *B*). One set comprises residues in the IF domain, which also showed the largest changes in chemical shift values in NMR titration experiments with substrates [12,25]. The second set is located in the FKBP domain with the majority close to the PPIase active site. We observed this slow motion for both free *Ec*SlyD* and for free *Tt*SlyD. This shows again the close dynamic coupling of both domains on the catalytic timescale. Surprisingly, the 100 s^{-1} fluctuations could not be detected by NMR relaxation. These fluctuations were revealed by smFRET using a pair of dyes attached to different domains with a Förster radius of 51 Å. We presume that these long-range fluctuations of both domains do not result in significant chemical shift differences between the open and closed states and thus no dispersion of the R_2 relaxation rates was observable on this timescale.

Again, the NMR experiments following inhibitor binding shed new light on the slow 1–10 s^{-1} dynamics observed in both domains, which was not observed in the smFRET experiments. Binding of Rapamycin

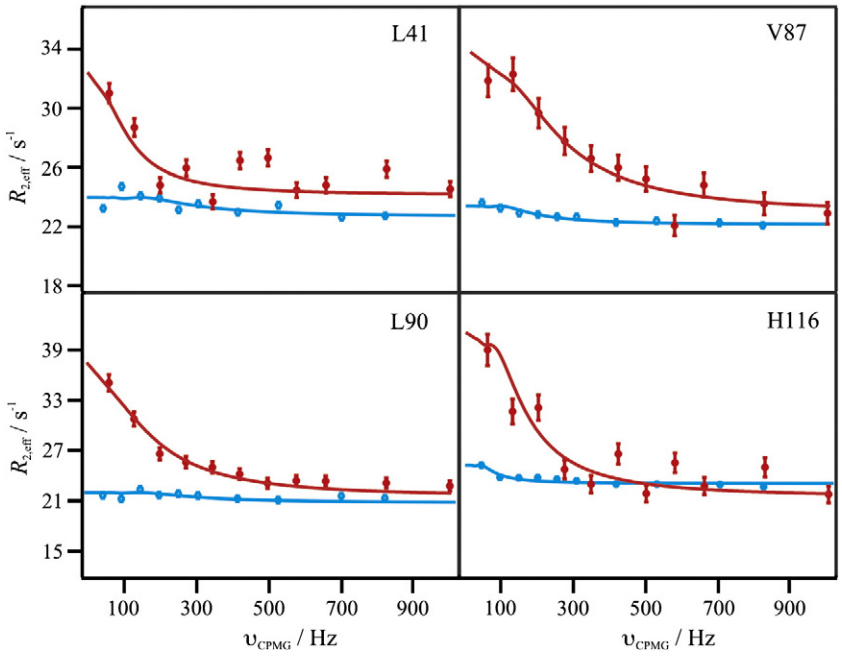

Fig. 6. Representative ^{15}N R_2 relaxation dispersion curves for *Ec*SlyD* (*open blue circles*) and *Ec*SlyD*Y68W (*solid red circles*) are shown for L41, V87, L90 and H116. Chemical exchange contributions, R_{ex}, of the whole molecule strongly depend on the aromatic side chain of amino acid position 68. Note that tyrosine 68 is part of the active site of PPIase in *Ec*SlyD*. The kinetic exchange rate, k_{ex}, between two conformations (the simplest exchange model) increases from about 1–10 s^{-1} (*Ec*SlyD*; see also Fig. S6 *A* and Table S1) to about 500 s^{-1} (*Ec*SlyD*Y68W; see also Fig. S7). The effective transversal relaxation rates, $R_{2,eff}$, presented were recorded at $T = 298$ K and a magnetic field strength of 14.1 T.

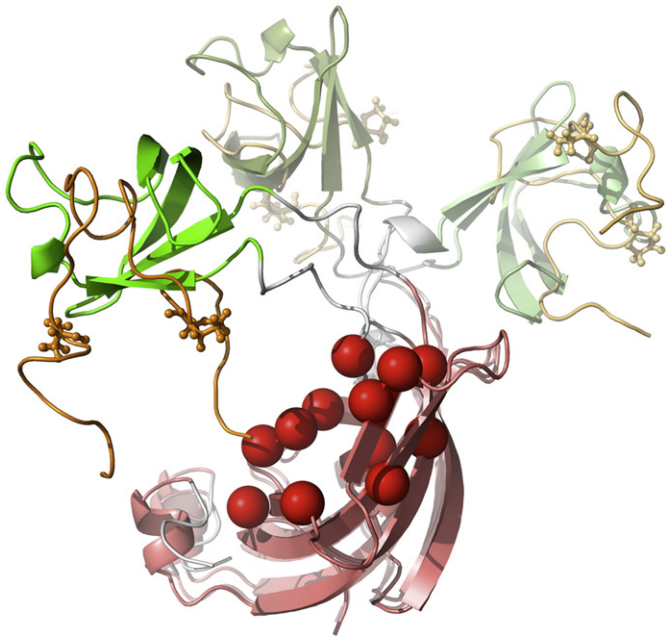

Fig. 7. Proposed model for the enzymatic mechanism of the prolyl isomerase SlyD. The substrates (unfolded polypeptides or proteins shown in brown) predominantly bind to the IF domain (shown in green). From the dynamic coupling between both domains we propose that upon opening and closing, the substrate is continuously exposed to the active and inhibitor-binding sites of the prolyl-peptidyl *cis-trans* isomerase, indicated by red spheres. This allows sampling of different conformations before the much slower product release step. The figure was prepared using PyMol (DeLano Scientific LLC, 2006).

occurs solely to the FKBP domain as shown by chemical shift mapping. This binding changed the dispersion of the ^{15}N R_2 relaxation rates of residues in the remote IF domain, the exchange contribution R_{ex} vanishes. This feedback shows that the slow dynamics observed in both domains originate from a common process. The synchronized timing between catalytic turnover and conformational exchange seen for wild type enzyme is lost as the catalytic efficiency – upon inhibitor interaction – drops down. We discovered earlier a similar dynamic coupling of both domains upon substrate-binding of Tat signal peptides, which was also not obvious from pure chemical shift mapping [25]. These peptides only bind to the IF domain but increase the local flexibility for the site of peptidyl-prolyl *cis*/*trans*-isomerization in the FKBP domain on the ps-to-ns timescale.

This crosstalk between chaperone and PPIase domain is further emphasized by the present finding that an amino acid exchange of tyrosine 68 within the PPIase site in the FKBP domain strongly affected both the catalytic efficiency of the enzyme and the ^{15}N R_2 relaxation dispersion, again in both domains. The substrate affinity during catalysis is reflected by the Michaelis–Menten constant K_M. It is similar for native *Ec*SlyD* and for the Y68W variant in the FKBP domain (Table S2), supporting the initial step of the model, which is substrate binding to the remote IF domain. However, tryptophan at position 68 reduces the maximal turnover number k_{cat} 30-fold by modifying the PPIase active site. In our model, this corresponds to a much longer sampling phase during opening and closing of SlyD before substrate release. The residues of both domains sense this single amino acid substitution by an enhanced dispersion amplitude of the ^{15}N R_2 rates compared to wild type *Ec*SlyD* which underlines again the dynamic crosstalk between both domains. A global understanding of the Y68 substitution on the entire catalytic cycle requires future experiments.

In conclusion, the combined application of various biophysical methods allowed us to generate a detailed model for the dynamic control underlying the SlyD catalytic mechanism. The model provides explanations at molecular levels for the Michaelis–Menten parameters K_M and k_{cat}. The interpretation of alterations in biochemical parameters by studying the local molecular motions using NMR relaxation studies has so far proved successful for many single-domain proteins [29–31,58–60]. It has also been useful in unraveling rate-limiting steps during catalysis [61]. Many enzymes reveal a multi-domain topology, which modulates the catalytic efficiency of the active site. The effects of these domains on catalytic efficiency can be more comprehensively explained by including the dynamics of the systems. For dual-domain proteins such as SlyD, this has so far been rarely reported [62].

Acknowledgments

This research was supported by grants from the DFG (SFB 610, GRK 1026). Significant investments into the NMR facility from the European Regional Development Fund (ERDF) by the European Union are also gratefully acknowledged. We additionally thank Ulrich Weininger, Christian G. Hübner, Dana Kahra, Caroline Haupt, Christian Löw and Franz X. Schmid for very fruitful discussions and Christian G. Hübner and Dana Kahra for preparation of Fig. 7. We are grateful to Gary Sawers for carefully reading of this manuscript.

Appendix A. Supplementary data

Supplementary data to this article can be found online at http://dx.doi.org/10.1016/j.bpc.2012.11.003.

References

[1] W.D. Roof, S.M. Horne, K.D. Young, R. Young, SlyD, a host gene required for phi X174 lysis, is related to the FK506-binding protein family of peptidyl-prolyl cis-trans-isomerases, Journal of Biological Chemistry 269 (1994) 2902–2910.
[2] G. Fischer, Peptidyl-prolyl *cis/trans* isomerases and their effectors, Angewandte Chemie, International Edition 33 (1994) 1415–1436.
[3] C. Haupt, C. Löw, M.T. Stubbs, J. Balbach, Metallochaperone SlyD. in: R.A. Scott (Ed.), Encyclopedia of Inorganic and Bioinorganic Chemistry (online), John Wiley & Sons, Ltd., 2012, http://dx.doi.org/10.1002/9781119951438.eibc2061.
[4] C. Scholz, B. Eckert, F. Hagn, P. Schaarschmidt, J. Balbach, F.X. Schmid, SlyD proteins from different species exhibit high prolyl isomerase and chaperone activities, Biochemistry 45 (2006) 20–33.
[5] S. Hottenrott, T. Schumann, A. Plückthun, G. Fischer, J.U. Rahfeld, The *Escherichia coli* SlyD is a metal ion-regulated peptidyl-prolyl cis/trans-isomerase, Journal of Biological Chemistry 272 (1997) 15697–15701.
[6] T.A. Knappe, B. Eckert, P. Schaarschmidt, C. Scholz, F.X. Schmid, Insertion of a chaperone domain converts FKBP12 into a powerful catalyst of protein folding, Journal of Molecular Biology 368 (2007) 1458–1468.
[7] H. Kaluarachchi, D.E.K. Sutherland, A. Young, I.J. Pickering, M.J. Stillman, D.B. Zamble, The Ni(II)-binding properties of the metallochaperone SlyD, Journal of the American Chemical Society 131 (2009) 18489–18500.
[8] K.C. Chung, D.B. Zamble, The *Escherichia coli* metal-binding chaperone SlyD interacts with the large subunit of [NiFe]-hydrogenase 3, FEBS Letters 585 (2011) 291–294.
[9] W. Graubner, A. Schierhorn, T. Bruser, DnaK plays a pivotal role in Tat targeting of CueO and functions beside SlyD as a general Tat signal binding chaperone, Journal of Biological Chemistry 282 (2007) 7116–7124.
[10] C. Löw, P. Neumann, H. Tidow, U. Weininger, C. Haupt, B. Friedrich-Epler, C. Scholz, M.T. Stubbs, J. Balbach, Crystal structure determination and functional characterization of the metallochaperone SlyD from *Thermus thermophilus*, Journal of Molecular Biology 398 (2010) 375–390.
[11] L. Martino, Y. He, K.L.D. Hands-Taylor, E.R. Valentine, G. Kelly, C. Giancola, M.R. Conte, The interaction of the *Escherichia coli* protein SlyD with nickel ions illuminates the mechanism of regulation of its peptidyl-prolyl isomerase activity, FEBS Journal 276 (2009) 4529–4544.
[12] U. Weininger, C. Haupt, K. Schweimer, W. Graubner, M. Kovermann, T. Brüser, C. Scholz, P. Schaarschmidt, G. Zoldak, F.X. Schmid, J. Balbach, NMR solution structure of SlyD from *Escherichia coli*: spatial separation of prolyl isomerase and chaperone function, Journal of Molecular Biology 387 (2009) 295–305.
[13] T. Cheng, H. Li, W. Xia, H. Sun, Multifaceted SlyD from *Helicobacter pylori*: implication in [NiFe] hydrogenase maturation, Journal of Biological Inorganic Chemistry (2011), http://dx.doi.org/10.1007/s00775-00011-00855-y.
[14] G. Fischer, B. Wittmann-Liebold, K. Lang, T. Kiefhaber, F.X. Schmid, Cyclophilin and peptidyl-prolyl-cis/trans-isomerase are probably identical proteins, Nature 337 (1989) 476–478.
[15] S.T. Park, R.A. Aldape, O. Futer, M.T. Decenzo, D.J. Livingston, PPIase catalysis by human FK506-binding protein proceeds through a conformational twist mechanism, Journal of Biological Chemistry 267 (1992) 3316–3324.
[16] A. Galat, S.M. Metcalfe, Peptidylproline cis/trans isomerases, Progress in Biophysics and Molecular Biology 63 (1995) 67–118.

[17] M. Weiwad, A. Werner, P. Rucknagel, A. Schierhorn, G. Kullertz, G. Fischer, Catalysis of proline-directed protein phosphorylation by peptidyl-prolyl cis/trans isomerases, Journal of Molecular Biology 339 (2004) 635–646.
[18] R. Suzuki, K. Nagata, F. Yumoto, M. Kawakami, N. Nemoto, M. Furutani, K. Adachi, T. Maruyama, M. Tanokura, Three-dimensional solution structure of an archaeal FKBP with a dual function of peptidyl prolyl cis-trans isomerase and chaperone-like activities, Journal of Molecular Biology 328 (2003) 1149–1160.
[19] S. Walter, J. Buchner, Molecular chaperones—cellular machines for protein folding, Angewandte Chemie, International Edition 41 (2002) 1098–1113.
[20] J.C. Young, V.R. Agashe, K. Siegers, F.U. Hartl, Pathways of chaperone-mediated protein folding in the cytosol, Nature Reviews. Molecular Cell Biology 5 (2004) 781–791.
[21] B. Bukau, E. Deuerling, C. Pfund, E.A. Craig, Getting newly synthesized proteins into shape, Cell 101 (2000) 119–122.
[22] G. Zoldak, L. Carstensen, C. Scholz, F.X. Schmid, Consequences of domain insertion on the stability and folding mechanism of a protein, Journal of Molecular Biology 386 (2009) 1138–1152.
[23] G. Fischer, H. Bang, E. Berger, A. Schellenberger, Conformational specificity of chymotrypsin toward proline-containing substrates, Biochimica et Biophysica Acta 791 (1984) 87–97.
[24] E. Holzapfel, M. Moser, E. Schiltz, T. Ueda, J.-M. Betton, M. Müller, Twin-arginine-dependent translocation of SufI in the absence of cytosolic helper proteins, Biochemistry 48 (2009) 5096–5105.
[25] M. Kovermann, R. Zierold, C. Haupt, C. Löw, J. Balbach, NMR relaxation unravels interdomain crosstalk of the two domain prolyl isomerase and chaperone SlyD, Biochimica et Biophysica Acta 1814 (2011) 873–881.
[26] H. Kaluarachchi, M. Altenstein, S.R. Sugumar, J. Balbach, D.B. Zamble, C. Haupt, Nickel binding and [NiFe]-hydrogenase maturation by the metallochaperone SlyD with a single metal-binding site in *Escherichia coli*, Journal of Molecular Biology 417 (2012) 28–35.
[27] D. Kahra, M. Kovermann, C. Löw, V. Hirschfeld, C. Haupt, J. Balbach, C.G. Hübner, Conformational plasticity and dynamics in the generic protein folding catalyst SlyD unraveled by single-molecule FRET, Journal of Molecular Biology 411 (2011) 781–790.
[28] R.P. Jakob, G. Zoldak, T. Aumüller, F.X. Schmid, Chaperone domains convert prolyl isomerases into generic catalysts of protein folding, Proceedings of the National Academy of Sciences 106 (2009) 20282–20287.
[29] D.D. Boehr, D. McElheny, H.J. Dyson, P.E. Wright, The dynamic energy landscape of dihydrofolate reductase catalysis, Science 313 (2006) 1638–1642.
[30] E.Z. Eisenmesser, D.A. Bosco, M. Akke, D. Kern, Enzyme dynamics during catalysis, Science 295 (2002) 1520–1523.
[31] E.Z. Eisenmesser, O. Millet, W. Labeikovsky, D.M. Korzhnev, M. Wolf-Watz, D.A. Bosco, J.J. Skalicky, L.E. Kay, D. Kern, Intrinsic dynamics of an enzyme underlies catalysis, Nature 438 (2005) 117–121.
[32] K. Henzler-Wildman, D. Kern, Dynamic personalities of proteins, Nature 450 (2007) 964–972.
[33] Y.W. Bai, J.S. Milne, L. Mayne, S.W. Englander, Protein stability parameters measured by hydrogen exchange, Proteins: Structure Function and Genetics 20 (1994) 4–14.
[34] N.A.J. van Nuland, V. Forge, J. Balbach, C.M. Dobson, Real-time NMR studies of protein folding, Accounts of Chemical Research 31 (1998) 773–780.
[35] Z. Luz, S. Meiboom, Nuclear magnetic resonance study of the protolysis of trimethylammonium ion in aqueous solution—order of the reaction with respect to solvent, Journal of Chemical Physics 39 (1963) 366–370.
[36] J.P. Loria, M. Rance, A.G. Palmer, A relaxation-compensated Carr–Purcell–Meiboom–Gill sequence for characterizing chemical exchange by NMR spectroscopy, Journal of the American Chemical Society 121 (1999) 2331–2332.
[37] M. Tollinger, N.R. Skrynnikov, F.A. Mulder, J.D. Forman-Kay, L.E. Kay, Slow dynamics in folded and unfolded states of an SH3 domain, Journal of the American Chemical Society 123 (2001) 11341–11352.
[38] J. Schlegel, G.S. Armstrong, J.S. Redzic, F. Zhang, E.Z. Eisenmesser, Characterizing and controlling the inherent dynamics of cyclophilin-A, Protein Science 18 (2009) 811–824.
[39] A.T. Namanja, X.J. Wang, B. Xu, A.Y. Mercedes-Camacho, B.D. Wilson, K.A. Wilson, F.A. Etzkorn, J.W. Peng, Toward flexibility–activity relationships by NMR spectroscopy: dynamics of Pin1 ligands, Journal of the American Chemical Society 132 (2010) 5607–5609.
[40] L.M. Mayr, O. Landt, U. Hahn, F.X. Schmid, Stability and folding kinetics of ribonuclease T1 are strongly altered by the replacement of cis-proline 39 with alanine, Journal of Molecular Biology 231 (1993) 897–912.
[41] M. Mücke, F.X. Schmid, Folding mechanism of ribonuclease T1 in the absence of the disulfide bonds, Biochemistry 33 (1994) 14608–14619.
[42] M. Mücke, F.X. Schmid, Intact disulfide bonds decelerate the folding of ribonuclease T1, Journal of Molecular Biology 239 (1994) 713–725.
[43] J. Weigelt, Single scan, sensitivity- and gradient-enhanced TROSY for multidimensional NMR experiments, Journal of the American Chemical Society 120 (1998) 10778–10779.
[44] J.P. Carver, R.E. Richards, A general two-site solution for the chemical exchange produced dependence of T2 upon the Carr–Purcell pulse separation, Journal of Magnetic Resonance 6 (1972) 89–105.
[45] S. Mori, C. Abeygunawardana, M.O. Johnson, P.C. van Zijl, Improved sensitivity of HSQC spectra of exchanging protons at short interscan delays using a new fast HSQC (FHSQC) detection scheme that avoids water saturation, Journal of Magnetic Resonance. Series B 108 (1995) 94–98.
[46] F. Delaglio, S. Grzesiek, G.W. Vuister, G. Zhu, J. Pfeifer, A. Bax, NMRPipe: a multidimensional spectral processing system based on UNIX pipes, Journal of Biomolecular NMR 6 (1995) 277–293.
[47] B.A. Johnson, R.A. Blevins, NMRView: a computer program for visualization and analysis of NMR data, Journal of Biomolecular NMR 4 (1994) 603–614.
[48] M.R. Eftink, Fluorescence methods for studying equilibrium macromolecule-ligand interactions, Methods in Enzymology 278 (1997) 221–257.
[49] M. Zeeb, J. Balbach, Single-stranded DNA binding of the cold shock protein CspB from Bacillus subtilis: NMR mapping and mutational characterisation, Protein Science 12 (2003) 112–123.
[50] H. Gutfreund, Kinetics for the Life Sciences, University Press, Cambridge, 1998.
[51] H. Fretz, M.W. Albers, A. Galat, R.F. Standaert, W.S. Lane, S.J. Burakoff, B.E. Bierer, S.L. Schreiber, Rapamycin and FK506 binding proteins (immunophilins), Journal of the American Chemical Society 113 (1991) 1409–1411.
[52] J.Y. Chang, S.N. Sehgal, C.C. Bansbach, FK506 and Rapamycin — novel pharmacological probes of the immune response, Trends in Pharmacological Sciences 12 (1991) 218–223.
[53] B.E. Bierer, P.S. Mattila, R.F. Standaert, L.A. Herzenberg, S.J. Burakoff, G. Crabtree, S.L. Schreiber, Two distinct signal transmission pathways in lymphocytes-T are inhibited by complexes formed between an immunophilin and either FK506 or Rapamycin, Proceedings of the National Academy of Sciences 87 (1990) 9231–9235.
[54] C.A. Lepre, J.A. Thomson, J.M. Moore, Solution structure of FK506 bound to FKBP-12, FEBS Letters 302 (1992) 89–96.
[55] T.J. Wandless, S.W. Michnick, M.K. Rosen, M. Karplus, S.L. Schreiber, FK506 and Rapamycin binding to FKBP — common elements in immunophilin ligand complexation, Journal of the American Chemical Society 113 (1991) 2339–2341.
[56] T. Ikura, N. Ito, Requirements for peptidyl-prolyl isomerization activity: a comprehensive mutational analysis of the substrate-binding cavity of FK506-binding protein 12, Protein Science 16 (2007) 2618–2625.
[57] C. Haupt, U. Weininger, M. Kovermann, J. Balbach, Local and coupled thermodynamic stability of the two domain and bifunctional enzyme SlyD from *Escherichia coli*, Biochemistry 50 (2011) 7321–7329.
[58] K.A. Henzler-Wildman, M. Lei, V. Thai, S.J. Kerns, M. Karplus, D. Kern, A hierarchy of timescales in protein dynamics is linked to enzyme catalysis, Nature 450 (2007) 913–916.
[59] K.A. Henzler-Wildman, V. Thai, M. Lei, M. Ott, M. Wolf-Watz, T. Fenn, E. Pozharski, M.A. Wilson, G.A. Petsko, M. Karplus, C.G. Hubner, D. Kern, Intrinsic motions along an enzymatic reaction trajectory, Nature 450 (2007) 838–844.
[60] G. Bhabha, J. Lee, D.C. Ekiert, J. Gam, I.A. Wilson, H.J. Dyson, S.J. Benkovic, P.E. Wright, A dynamic knockout reveals that conformational fluctuations influence the chemical step of enzyme catalysis, Science 332 (2011) 234–238.
[61] V.Y. Torbeev, H. Raghuraman, D. Hamelberg, M. Tonelli, W.M. Westler, E. Perozo, S.B.H. Kent, Protein conformational dynamics in the mechanism of HIV-1 protease catalysis, Proceedings of the National Academy of Sciences 108 (2011) 20982–20987.
[62] J.H. Cho, V. Muralidharan, M. Vila-Perello, D.P. Raleigh, T.W. Muir, A.G. Palmer, Tuning protein autoinhibition by domain destabilization, Nature Structural & Molecular Biology 18 (2011) 550–555.